

Surface reconstructions of InSb(100) observed by scanning tunneling microscopy

C. F. McConville*

Department of Physics, University of Warwick, Coventry CV4 7AL, United Kingdom

T. S. Jones

*Department of Chemistry and Interdisciplinary Research Centre for Semiconductor Materials,
Imperial College, London SW7 2AY, United Kingdom*

F. M. Leibsle and S. M. Driver†

Surface Science Research Centre, University of Liverpool, Liverpool L69 3BX, United Kingdom

T. C. Q. Noakes

Department of Physics, University of Warwick, Coventry CV4 7AL, United Kingdom

M. O. Schweitzer and N. V. Richardson

Surface Science Research Centre, University of Liverpool, Liverpool L69 3BX, United Kingdom

(Received 9 May 1994)

A number of surface reconstructions formed on InSb(100) have been observed with atomic resolution using scanning tunneling microscopy (STM). Cycles of low-energy ion bombardment and annealing result in the formation of an In-rich surface with a $c(8\times 2)$ diffraction pattern. Filled-states images of this indicate a (4×1) periodicity arising from imaging occupied lone-pair orbitals on exposed second-layer Sb atoms. The controlled deposition of Sb_4 from a Knudsen effusion source onto the $c(8\times 2)$ surface at elevated temperatures led to the formation of a (1×1) , $c(4\times 4)$, and an asymmetric (1×3) structure, in order of decreasing Sb/In ratio. Filled- and empty-states STM images of all these Sb-rich reconstructions were generated and the coexistence of the different structures was also observed. Both the (1×1) and asymmetric (1×3) surfaces showed a high degree of disorder while the $c(4\times 4)$ surface was highly ordered. The $c(4\times 4)$ structure, which involves the chemisorption of Sb onto an already Sb-terminated surface, is characterized by blocks of three pairs of well-resolved Sb dimers. Structural models are proposed for the ordered structures observed.

I. INTRODUCTION

In recent years there has been increasing interest, both for fundamental and technological reasons, in the growth of InSb by techniques such as molecular-beam epitaxy (MBE). Technological applications of this narrow-band-gap III-V material include use as infrared sensors and detectors and also for high-speed quantum-well devices due to the small effective mass and high mobility of electrons in this material.¹⁻³ Epitaxial growth is most commonly carried out on the (100) surface. Consequently, it is necessary to understand the details of the possible structures formed in the production of contamination-free, well-ordered surfaces for subsequent MBE growth.

The most common method used to produce clean, ordered InSb(100) surfaces is a combination of inert gas ion bombardment and annealing procedures. This is necessary because the low melting point of InSb means that the desorption temperature of the native oxide lies extremely close to the melting point of the bulk material (800 K) and well above its noncongruent temperature (~ 620 K). Although ion bombardment is successful in producing chemically clean surfaces, it is apparent that structural damage, lattice imperfections, and changes in the surface stoichiometry, which are associated with the process, cannot be completely eliminated by thermal an-

nealing. Preferential depletion of the group-V species results in the formation of defects which dramatically effect the electronic properties of the near-surface region of the material.⁴⁻⁷ Postbombardment annealing of the InSb(100) surface results in a more ordered surface as detected by low-energy electron diffraction (LEED).^{4,5,8,9} Annealing to ~ 500 K results in the formation of a (4×1) LEED pattern with streaking between the rows of the $\frac{1}{4}$ -order fractional spots,^{8,9} while higher-temperature annealing (> 600 K) leads to the formation of a sharper $c(8\times 2)$ pattern.^{4,5} This latter structure has also been observed in both reflection high-energy electron-diffraction (RHEED) (Refs. 10 and 11) and high-energy electron-diffraction (HEED) (Ref. 12) studies of MBE-grown InSb(100) under In-rich growth conditions.

In common with all the (100) surfaces of III-V semiconductor compounds, a number of other surface reconstructions can be formed by InSb depending on the Sb/In surface ratio and the substrate temperature (Fig. 1). Those reconstructions studied during epitaxial growth are all Sb-terminated and include a (1×1) , an asymmetric (1×3) , a (4×3) , a (7×5) , and a $c(4\times 4)$ structure.¹⁰⁻¹² Although some of these reconstructions are similar to those formed on the more commonly studied GaAs(100) surface, there is one important difference in that no phase diagram has been mapped, or is known to

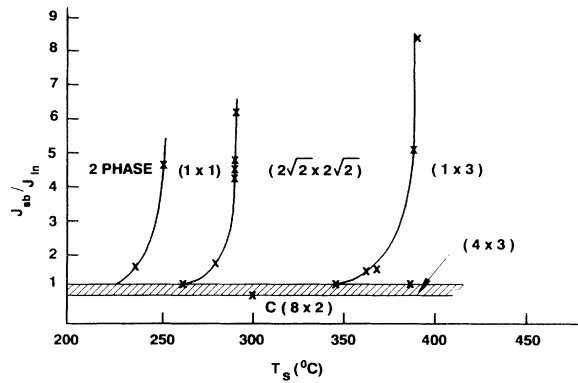


FIG. 1. Phase diagram for the surface reconstructions observed on InSb(100) as a function of the Sb/In arrival rate and the surface temperature.

exist in equilibrium, for the GaAs(100) surface. Hence it is more difficult to unambiguously identify large areas of a single reconstruction under static conditions on this surface. In contrast, all of the InSb(100) reconstructions observed are also stable for a given static Sb/In ratio, allowing each one to be produced in turn on the surface.^{13–15}

Although surface diffraction techniques have so far been used to provide structural information regarding the different surface reconstructions formed, it is becoming increasingly apparent that scanning tunneling microscopy (STM) offers unique details at the atomic scale. Images of the (100) surface of MBE-grown GaAs, for example, have provided direct evidence for several of the models for the surface reconstructions proposed on the basis of earlier experimental diffraction and spectroscopic studies.¹⁶ Specific emphasis has been placed on the As-terminated (2×4) surface, in which atomic resolution images are dominated by unit cells containing two As dimers,^{17,18} although three dimers per unit cell have also been observed.¹⁹ Relatively little attention has so far been directed at the reconstructions formed on the (100) surfaces of other III-V semiconductor materials. This is in contrast to STM studies of the cleaved (110) surfaces, where studies of both GaAs (Ref. 20) and InSb (Ref. 21) indicate that Ga (In) and As (Sb) atoms are imaged, respectively, under conditions of positive and negative bias.

In this paper we present a detailed atomic resolution STM study of a number of reconstructions formed on InSb(100), focusing in particular on the In-terminated $c(8 \times 2)$ structure and the Sb-terminated (1×1) , $c(4 \times 4)$, and asymmetric (1×3) structures. The $c(8 \times 2)$ and $c(4 \times 4)$ structures are found to be highly ordered, while the (1×1) and asymmetric (1×3) show evidence of considerable disorder at the atomic scale. In particular, our images show direct evidence of the existence of Sb-Sb bonding on the InSb(100)- $c(4 \times 4)$ surface. This is consistent with groups of three Sb-Sb pairs arranged in a so-called missing-dimer model, previously used to describe the same reconstruction on GaAs(100), but observed here with much higher spatial resolution.

II. EXPERIMENT

The measurements were carried out in an UHV chamber equipped with LEED, Auger electron spectroscopy, STM (Omicron GmbH, Germany), and a fast entry load lock for efficient transfer of the samples. The InSb substrate surfaces (MCP Wafer Technology Ltd. UK) were oriented within 0.25° of the (100) plane. Each heavily doped *n*-type sample (Te doped, $n \sim 4 \times 10^{18} \text{ cm}^{-3}$) was cleaved from a 500- μm -thick wafer of bulk *n*-type material that had previously been mechanically and then electrochemically polished to remove the majority of the subsurface damage caused by the mechanical polishing process. Prior to insertion in vacuum, each sample ($\sim 10 \text{ mm}^2$) was chemically etched with a mixture of lactic, nitric, and hydrofluoric acids mixed in the ratio 25:4:1. This removed any residual surface damage and resulted in the formation of a stable oxide layer.²² The samples were each mounted onto a molybdenum plate, shaped to fit the STM, and held in place by thin tantalum foil strips spot welded to the plate. Sample heating was achieved radiatively using a filament mounted behind the molybdenum plate, with the temperature being monitored by a chromel-alumel thermocouple. Each sample was outgassed for approximately 1 h at 600 K and then cleaned by three cycles of low-energy argon-ion bombardment (500 eV, 45° incidence angle, 1 h) each cycle followed by annealing to 650 K for 1 h.²³ This resulted in the formation of a sharp $c(8 \times 2)$ LEED pattern.^{5,9,15}

The antimony-rich surfaces were all formed by the controlled deposition of Sb_4 (quadruple zone refined, 6N pure elemental Sb) from a small Knudsen cell (WA Technology, UK) onto the InSb(100)- $c(8 \times 2)$ surface held at the appropriate substrate temperature. The substrate was held in the Sb flux for approximately 15 min. It was not possible to rotate the sample during Sb deposition. The Sb cell was then closed and the sample cooled to room temperature, where the LEED pattern of the desired reconstruction could be observed. In reproducing the phase diagram shown in Fig. 1, some slight variation in the temperatures, used to mark the transitions between each reconstruction, was observed. This was almost certainly due to the position of the thermocouple which was necessarily remote to allow sample transfer.

III. RESULTS AND DISCUSSION

The LEED patterns for the ordered reconstructions observed on InSb(100) are shown in Fig. 2. These diffraction patterns were all recorded at a primary electron energy of 47 eV and show the $c(8 \times 2)$, $c(4 \times 4)$, asymmetric (1×3) , and (1×1) structures in Figs. 2(a), 2(b), 2(c), and 2(d), respectively. In each case the diffraction pattern was shown to exist over the whole of the sample, and remained stable over periods of several hours. Although these structures are all linked, for the remainder of this paper the results and discussion will be split such that the STM images from each of the surface reconstructions can be considered in turn.

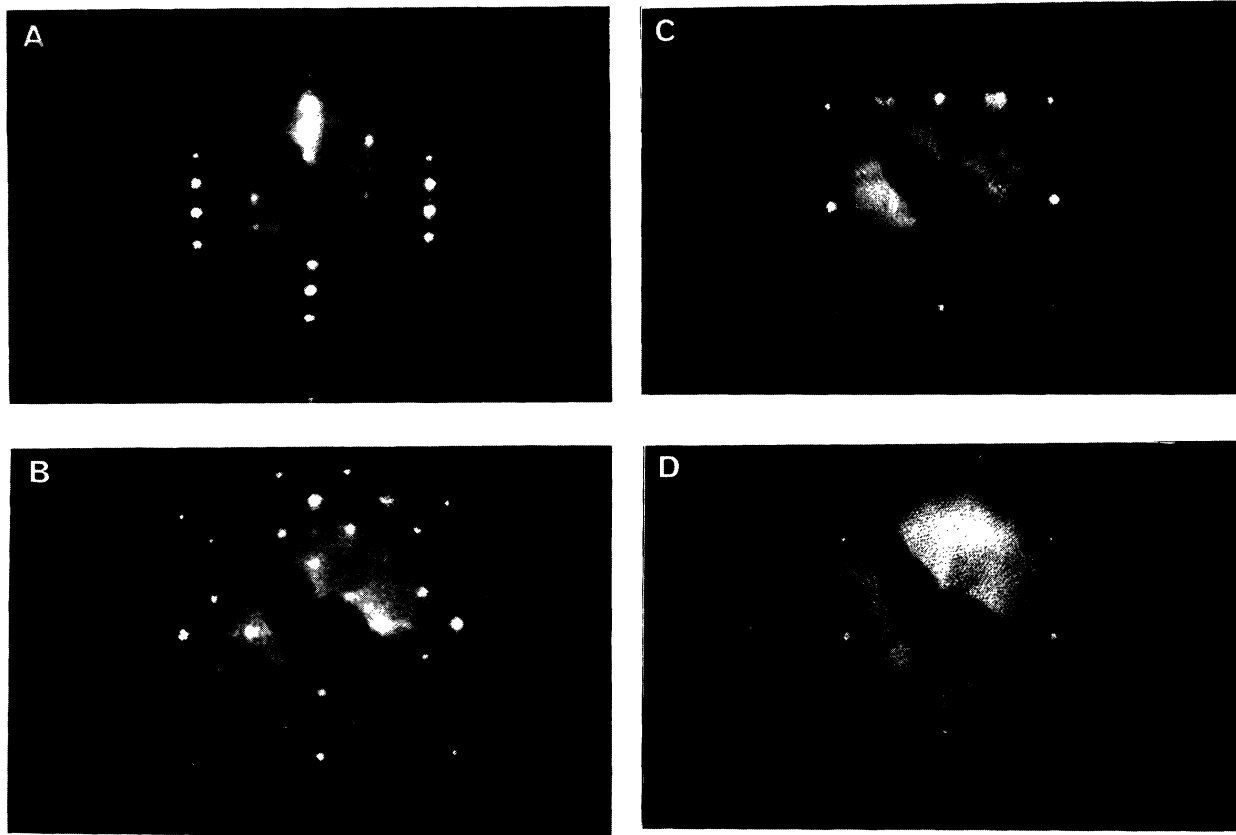


FIG. 2. LEED patterns of the various reconstructions formed on InSb(100): (a) the In-terminated $c(8 \times 2)$, and the Sb-terminated surfaces (b) $c(4 \times 4)$, (c) asymmetric (1×3) , and (d) (1×1) . The primary electron energy in each case was 47 eV.

A. The $c(8 \times 2)$ surface

A typical filled-states (-2 V sample bias, 1 nA tunnel current) STM topograph ($1500 \times 1500 \text{ \AA}^2$) of the InSb(100)- $c(8 \times 2)$ surface is shown in Fig. 3. Previous work has shown that at least three cycles of low-energy ion bombardment and annealing to ~ 650 K were required in order to produce a surface of this quality.²³ A large atomically flat terrace can be seen covering an area of the surface of about $1000 \times 1000 \text{ \AA}^2$ with smooth monatomic steps in both the top right and bottom right-hand corners of the image. The continuous parallel rows, oriented $\sim 45^\circ$ with respect to the $+x$ direction, are due to the occupied lone-pair orbitals of the antimony atoms. The medium-sized features ($< 100 \text{ \AA}$) on the surface are most probably excess In atoms, in small clusters, as a result of the preferential sputtering process.

A high-resolution filled-states (-3 V, 1 nA) image of this surface ($200 \times 200 \text{ \AA}^2$) is shown in Fig. 4. Although the LEED pattern [Fig. 2(a)] clearly exhibits a $c(8 \times 2)$ surface periodicity, the real-space STM image suggests a (4×1) periodicity as indicated by the unit cell shown in the image. Also, the alignment of step edges along the $[011]$ direction indicates that the (4×1) units are not staggered. Since the image in Fig. 4 involves tunneling

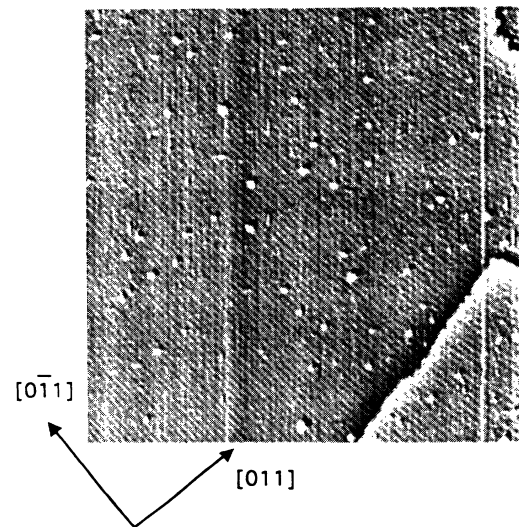


FIG. 3. A grey-scale STM topographic image ($1500 \times 1500 \text{ \AA}^2$) of the InSb(100)- $c(8 \times 2)$ surface produced after three cycles of argon-ion sputtering and annealing (650 K). Note the In droplets formed as a result of the ion bombardment. This image was produced using a sample bias of -2 V and a tunneling current of 1 nA.

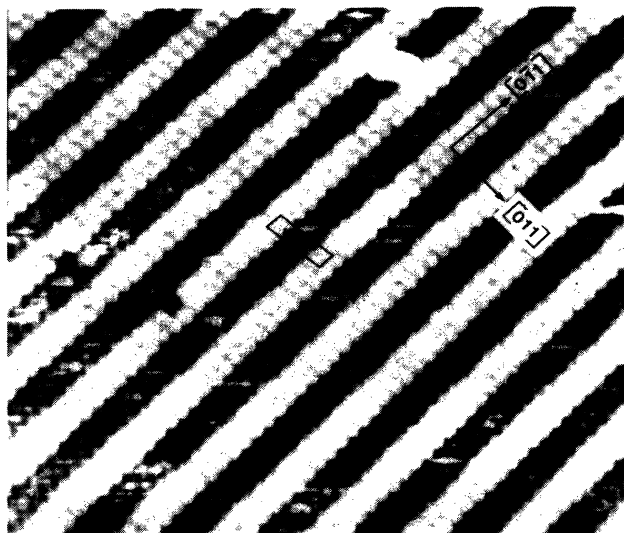


FIG. 4. A grey-scale STM topographic image ($200 \times 200 \text{ \AA}^2$) of the InSb(100)- $c(8 \times 2)$ surface after three cycles of argon-ion sputtering and annealing (650 K). The visible double rows are the occupied lone pair orbitals of second-layer Sb atoms. The (4×1) unit cell is indicated in the image which was recorded with a sample bias of -3 V and a tunneling current of 1 nA .

from filled states of the sample to unfilled states of the tip, the bright circular features observed arise from tunneling from occupied lone-pair orbitals of exposed Sb atoms in the *second layer* of the material and not from bonds associated with In atoms in the top surface layer.²⁴ Unsuccessful attempts were made to collect atomic resolution

empty-states images of this In-rich $c(8 \times 2)$ surface.

The apparent conflict between the (4×1) periodicity observed by STM and the $c(8 \times 2)$ periodicity seen in LEED can be resolved by considering the structural model originally proposed for this surface by John, Miller, and Chiang¹² on the basis of high-resolution core-level photoemission results. This missing-dimer model is shown in Fig. 5 and consists of $\frac{3}{4}$ of a monolayer of In dimers arranged in groups of three on top of a full monolayer Sb-terminated surface. The groups of three In dimers, whose bond axes are arranged parallel to each other and along the $[0\bar{1}1]$ azimuth, are separated by missing dimers in the $[011]$ direction in phase with other In-dimer groups in the direction of the bonds, but out of phase with dimer groups perpendicular to the bonds. The full translational symmetry of the surface is $c(8 \times 2)$, consistent with the LEED results. Closer inspection of this model can, however, rationalize the (4×1) symmetry indicated by STM. The location of the missing In dimers are such that one-half of the Sb atoms in the second layer are bonded to a single surface In atom rather than two. These exposed Sb atoms (at the corner of each block in Fig. 5) have a filled lone-pair orbital directed out of the surface into the vacuum. The tunneling conditions used to obtain the image shown in Fig. 4 are therefore those which select only these Sb atoms in the second layer. It is the arrangement of these atoms which then gives the (4×1) periodicity shown by STM.

In spite of the difficulties encountered attempting to collect empty-state images at atomic resolution on the In-terminated InSb(100) surface, there have been two reported STM studies of the equivalent Ga-terminated

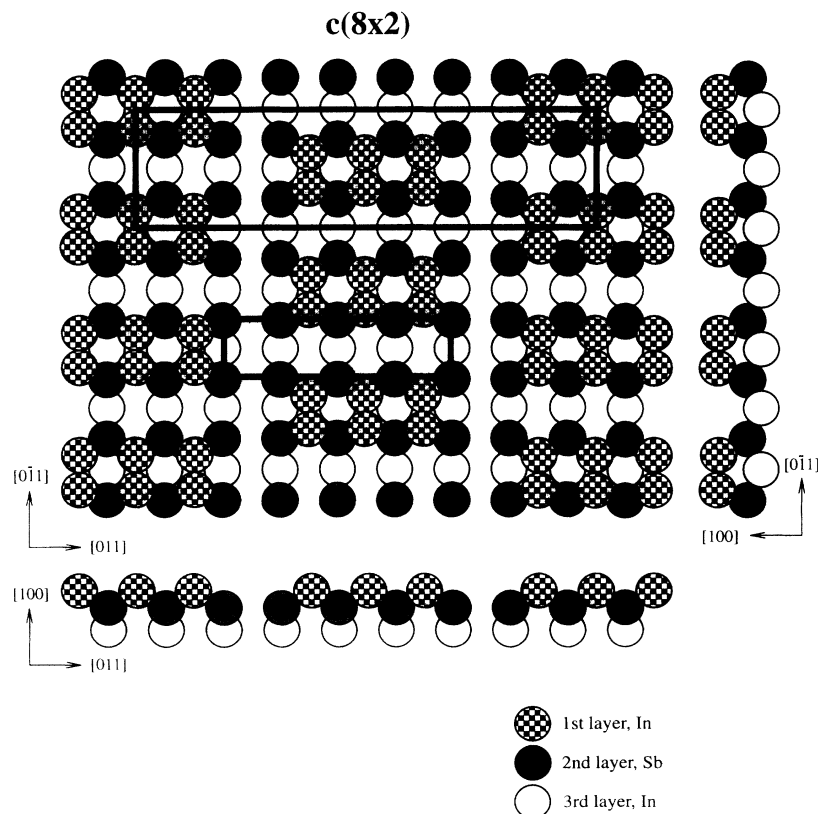


FIG. 5. A structural model for the InSb(100)- $c(8 \times 2)$ surface reconstruction. The (4×1) unit cell refers only to the Sb atoms in the second layer visible in the STM image, while the $c(8 \times 2)$ translational symmetry as seen by LEED takes into consideration the In dimers in the topmost surface layer.

structure formed on GaAs(100). Initial low-resolution work on MBE-grown material by Biegelsen *et al.*¹⁶ indicated a structure based on a missing gallium dimer model, in which the surface is composed of (4×2) subunits containing two adjacent Ga dimers and two missing dimers. More recent higher-resolution work, however, by Skala *et al.* [25] suggested that this surface is composed of equal numbers of gallium and arsenic atoms. They proposed a model in which the $c(8 \times 2)$ structure is formed from an ordered arrangement of (4×2) subunits, with each subunit containing two As and Ga dimers. Neither of these structures predicted for GaAs(100)- $c(8 \times 2)$ is consistent with the core-level photoemission data of John, Miller, and Chiang¹² for InSb(100)- $c(8 \times 2)$, or the STM image shown in Fig. 4.

B. The $c(4 \times 4)$ surface

The InSb(100)- $c(4 \times 4)$ surface was formed after deposition of Sb_4 at a substrate temperature of approximately 450 K. This structure could also be produced by Sb_4 deposition at room temperature followed by annealing to ~ 450 K. The LEED pattern for this surface is shown in Fig. 2(b) and demonstrates the full $(2\sqrt{2} \times 2\sqrt{2})R45^\circ$ translational symmetry. The corresponding filled-states $(-2.5$ V, 1 nA) STM image ($400 \times 400 \text{ \AA}^2$) consists of bright rectangular blocks, with the long direction of the rectangle aligned along the $[011]$ direction (Fig. 6). The equivalent empty-states image, over the same area of the sample ($400 \times 400 \text{ \AA}^2$), is shown in Fig. 8. The $c(4 \times 4)$ symmetry is clearly evident and the $(2\sqrt{2} \times 2\sqrt{2})R45^\circ$

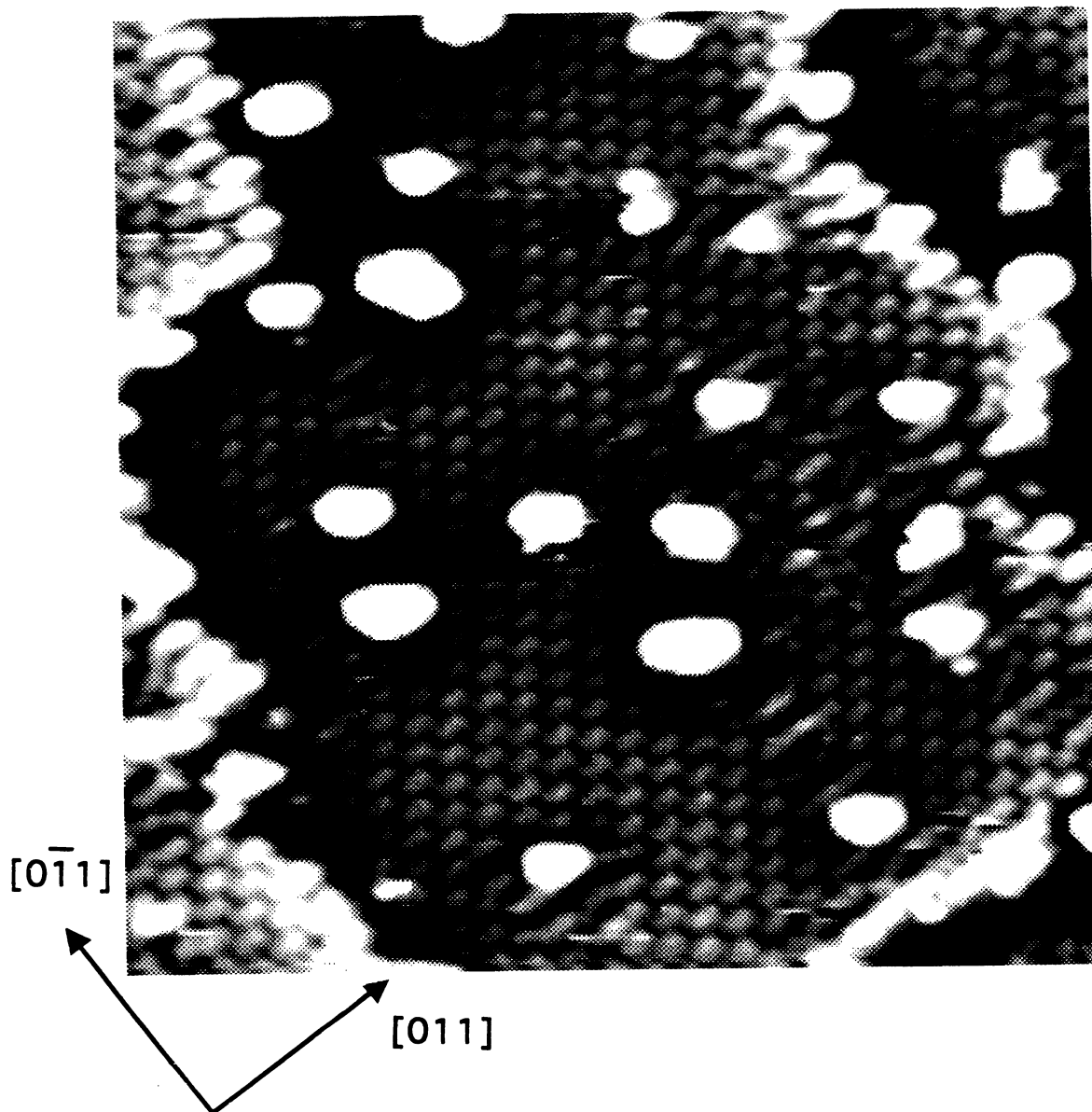


FIG. 6. A filled-states image ($400 \times 400 \text{ \AA}^2$) of the InSb(100)- $c(4 \times 4)$ surface, prepared by Sb_4 deposition onto the InSb(100)- $c(8 \times 2)$ surface held at a temperature of ~ 500 K. Note the “bricklike” blocks which are identified as Sb dimers. The image was recorded with a sample bias of -2.5 V and a tunnel current of 1 nA.

unit cell is shown on the image. It is also interesting to note that the bricklike structure appears to be more ordered in the case of the filled-state image (Fig. 6).

Higher-resolution STM images of this surface are shown in Fig. 7 and the inset to Fig. 8 for both filled- (-2.5 V, 1 nA) and empty-states ($+2.5$ V, 1 nA) imaging, respectively. Both of these images were recorded over the same area of the surface. They show identical features, namely that each of the bright rectangles is split into three individual sets of features which, in common with existing terminology, are assigned to Sb dimers with the dimer bond aligned along the $[0\bar{1}1]$ azimuthal direction.²⁴ The filled-states image clearly shows the individual Sb atoms within each dimer unit (Fig. 7). It is also noticeable that the central dimer in each block of three appears to have less electron density associated with it compared to the outer two dimer pairs. This suggests that it could be at a different height (i.e., lower in the surface) or that some electron density associated with the central dimer is transferred to the outer dimer pairs. This can be seen more clearly by comparing a complete block with one that has at least one missing Sb atom, and where, in every case, the central dimer appears brighter in the filled-state image shown. The number of blocks that contain one or more missing Sb atoms also accounts for the coverage range, in terms of Sb/In ratio, over which this structure is observed.

The images observed for this surface are similar to

those reported for MBE-grown GaAs(100)- $c(4\times 4)$ by Biegelse *et al.*¹⁶ and Tanaka *et al.*²⁶ The resolution of the Sb atoms making up the dimers is certainly better than the equivalent images observed for GaAs. This is most probably due to the InSb having a much larger lattice constant (6.4788 Å) compared with that of GaAs (5.6532 Å), resulting in a greater physical separation of the electron density associated with each Sb lone-pair orbital. Interestingly, Tanaka *et al.*²⁶ has also shown images for the GaAs(100)- $c(4\times 4)$ surface which suggest that the central dimer in each block may be at a different height compared with the outer dimer pairs.

A structural model consistent with our STM images for the InSb(100)- $c(4\times 4)$ surface is shown in Fig. 9. It was originally proposed on the basis of high-resolution core-level photoemission measurements for both GaAs (Ref. 27) and InSb.¹² This missing-dimer model consists of a top layer of Sb atoms, forming blocks of three so-called Sb dimers, located on top of a complete monolayer Sb-terminated surface. The bright features observed in both Figs. 7 and 8 under opposite bias, therefore correspond to tunneling both out of and into occupied and unoccupied molecular orbitals of the top-layer Sb atoms. The observation of the same species in both positive and negative sample bias is similar to recent results obtained by Wassermeier *et al.*²⁸ for GaAs(100)- (2×4) , and is consistent with the top surface layer [and in the case of the $c(4\times 4)$ structure also the second layer] containing

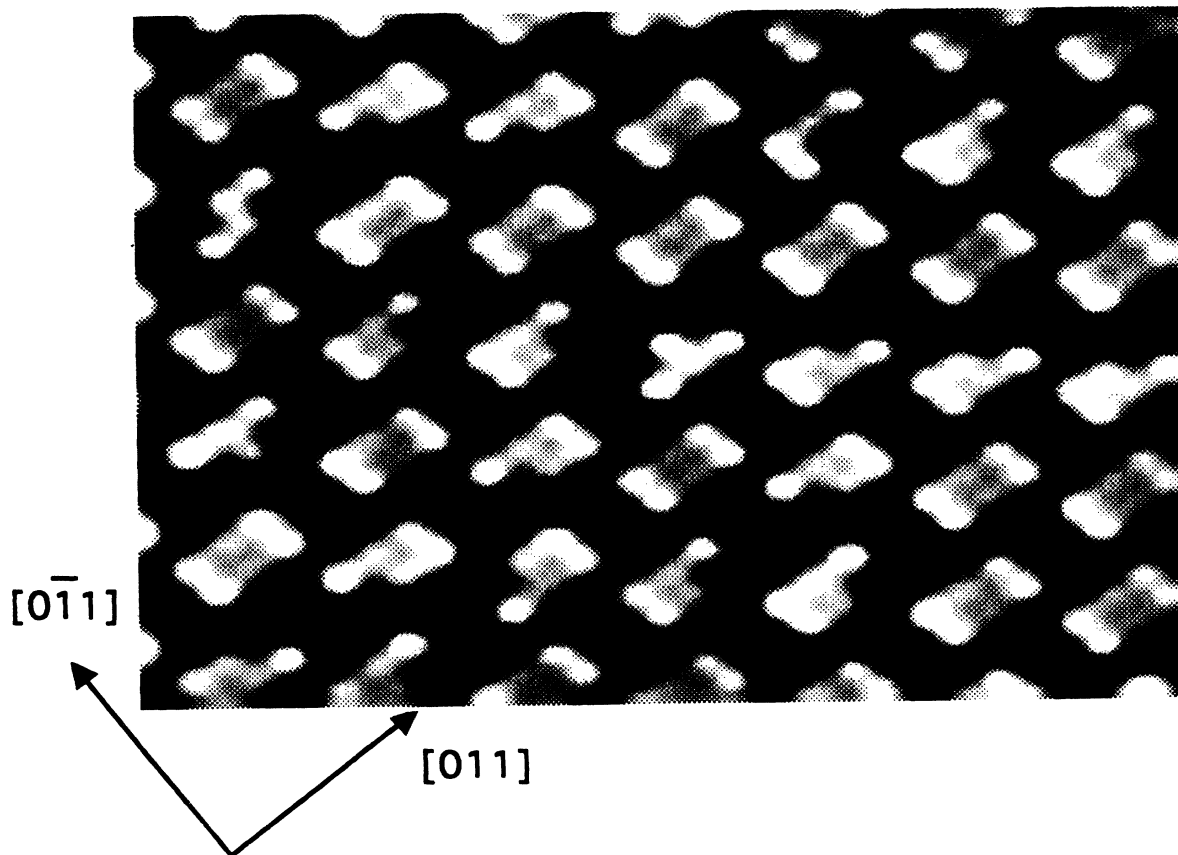


FIG. 7. A high-resolution filled-states image (105×70 Å²) of the InSb(100)- $c(4\times 4)$ surface showing the individual Sb atoms arranged in blocks of three dimers separated by a missing dimer. The $c(4\times 4)$, or $(2\sqrt{2}\times 2\sqrt{2})R45^\circ$, unit cell can clearly be seen by comparison with the model shown in Fig. 9. The image was recorded with a sample bias of -2.5 V and a tunneling current of 1 nA.

only group-V atoms. It has been shown for GaAs using thermal desorption, RHEED, and photoemission techniques that it is possible to produce the $c(4 \times 4)$ structure over a wide range of surface coverages, the only difference being the number of As atoms found in the surface layer.^{27,29} The structural model outlined in Fig. 9 is

consistent with the STM image shown for InSb (Fig. 7) and clearly shows blocks of six Sb atoms.

It is important to realize that the $c(4 \times 4)$ structure is fundamentally different from the other reconstructions formed on the (100) surface of these materials. This has led to a certain amount of confusion regarding the term

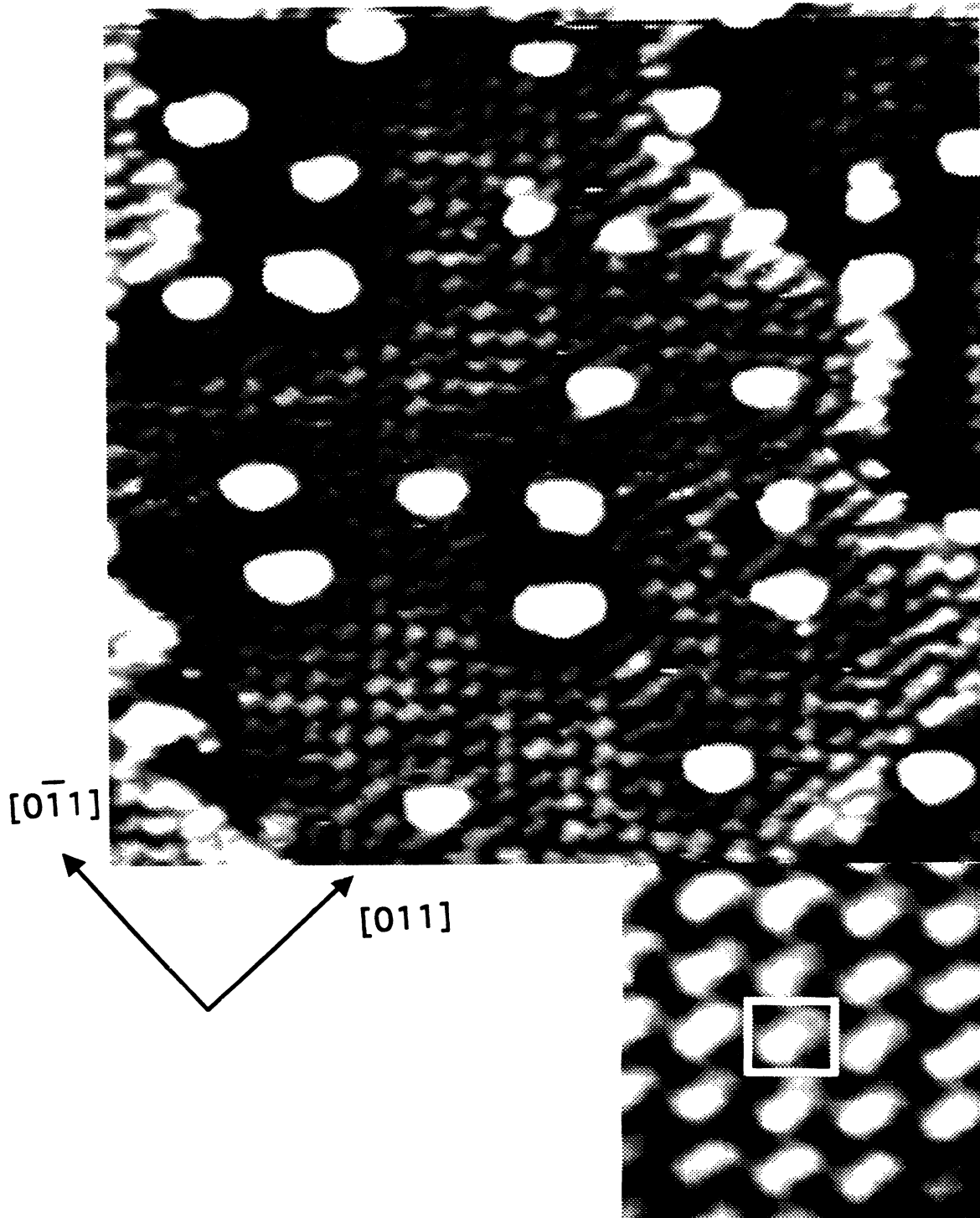


FIG. 8. An empty-states image ($400 \times 400 \text{ \AA}^2$) of the InSb(100)- $c(4 \times 4)$ surface, again showing Sb dimers arranged in blocks of three separated by a missing dimer. Note that the blocks, although identifiable, are less well resolved than in Fig. 7, even though the image was taken over the same area. The inset shows a region of the same surface at higher resolution. The image was recorded with a sample bias of +2.5 V and a tunneling current of 1 nA.

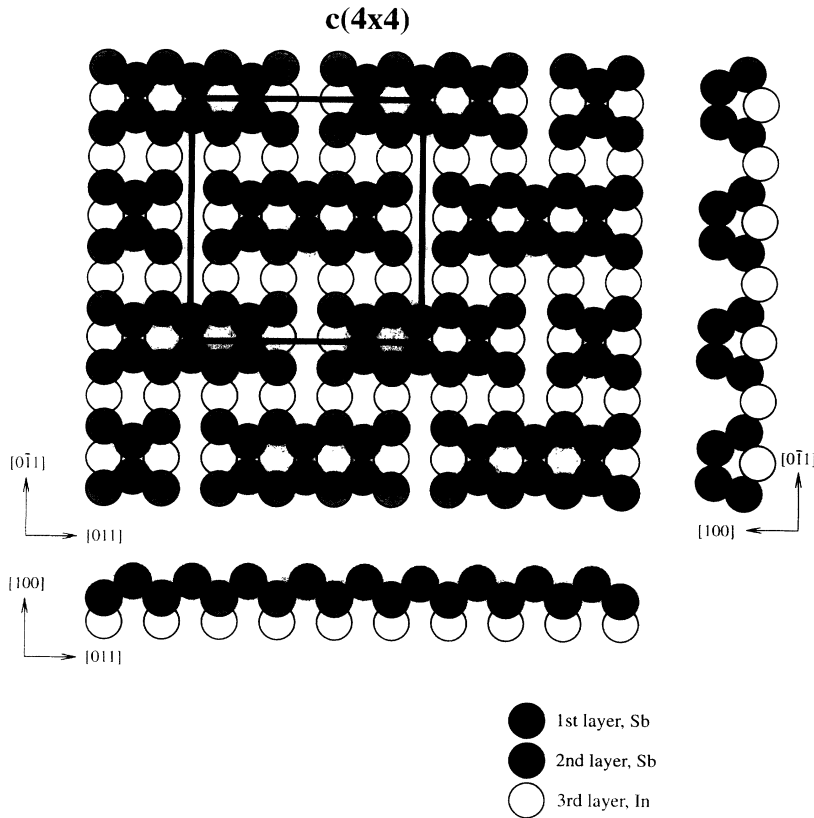


FIG. 9. A structural model for the Sb-terminated InSb(100)- $c(4 \times 4)$ surface. The model consists of 0.75-ML Sb atoms chemisorbed onto a full monolayer of Sb terminating the surface.

“dimer” when describing this structure which is formed on both InSb and GaAs.³⁰ All the group-V-terminated reconstructions, with the exception of the $c(4 \times 4)$ structure, involve the formation of group-V dimers in the top layer of the structure, with the group-V atoms in the surface bonded only to group-III atoms in the second layer. The $c(4 \times 4)$ structure, however, involves the chemisorption of excess group-V material onto an already group-V-terminated surface. Consequently, the surface consists of Sb atoms in the top layer that are bonded to the second layer of the structure *only* to Sb and *not* In atoms. This top layer of Sb atoms are therefore more indicative of bulk Sb bonding, with the atoms bonded to three other Sb atoms. Although it is common to describe the $c(4 \times 4)$ structure in terms of Sb (or As in the case of GaAs) dimers, the bonding arrangement at the surface means that they are fundamentally different from the dimers formed on the other surface reconstructions of these materials.³⁰

C. The asymmetric (1×3) surface

The asymmetric (1×3) surface of InSb(100) could be formed either by evaporation of Sb_4 onto InSb at a substrate temperature of ~ 500 K or, alternatively, by annealing the $c(4 \times 4)$ surface to 500 K in order to desorb some of the Sb. This structure has previously been studied using RHEED,^{10,11,31} HEED, core-level photoemission spectroscopy¹² and helium scattering.¹³ From the LEED pattern shown in Fig. 2(c), the source of the asymmetry in this reconstruction can clearly be seen. The initial identification of this asymmetric (1×3) phase

was made using RHEED, where the unequal spacing of the $\frac{1}{3}$ -order diffraction streaks was observed during MBE growth.^{10,11} A more accurate description of the LEED pattern shown in Fig. 2(c) might perhaps be as a (1×2) structure with split half-order spots.

A wide-scan grey-scale topographic image of the asymmetric (1×3) surface over an area of $(200 \times 130 \text{ \AA}^2)$ is shown in Fig. 10. This filled-state image (-2.75 V, 1

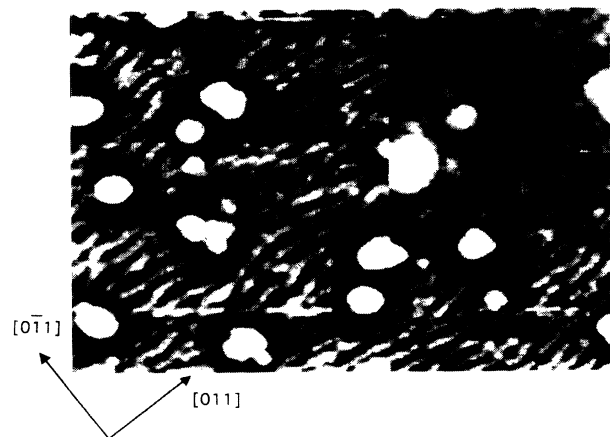


FIG. 10. A wide-area scan $(200 \times 130 \text{ \AA}^2)$ grey-scale topographic image of the asymmetric- (1×3) surface showing the Sb atoms aligned in short, “wormlike” chains along the $[011]$ direction. The high-resolution inset $(80 \times 50 \text{ \AA}^2)$ clearly shows the individual Sb atoms within each chain. The image was recorded with a bias voltage of -2.75 V and a tunnel current of 1 nA.

nÅ) indicates that the surface has significant shortrange disorder with Sb atoms aligned in short, "wormlike" chains essentially along the $[01\bar{1}]$ direction and separated by about 12 Å. The high-resolution image ($80 \times 50 \text{ \AA}^2$ inset to Fig. 10) clearly shows the individual Sb atoms within each chain. It is also notable that the length of the Sb chains vary in size from as small as three or four atoms to several tens of atoms in length ($\sim 10\text{--}200 \text{ \AA}$) and are abruptly terminated at the larger scale defects, which are most probably residual indium droplets.

The image shown in Fig. 10 is similar to that observed by Franklin *et al.*³² for the GaSb(100) symmetric (1×3) surface. Their model for this surface, based both on STM and photoemission data, is shown in Fig. 11 adapted for InSb. It consists of the unreconstructed In-terminated surface with two out of every three In rows along the $[0\bar{1}1]$ direction being replaced by Sb rows such that the neighboring Sb atoms dimerize in order to minimize the number of dangling bonds. Hence there is one-third of a monolayer of In and two-thirds of a monolayer of Sb in the top layer of the surface.

A generalized model for the asymmetric (1×3) reconstruction formed on InSb(100) has been proposed by de

Oliveira *et al.*³¹ They suggested that the asymmetric (1×3) structure is generated from the basic (2×4) structure by domain formation invoking the sequencing of two (2×4) unit cells of different Sb coverages, 0.75 and 0.50 ML, respectively. Using RHEED, they monitored the ratio of the separation of the two $\frac{1}{3}$ -order streaks and the separation of the integral-order streaks as a function of Sb coverage. This splitting fraction (F) was observed to decrease continuously with decreasing Sb coverage (increasing substrate temperature) such that, at close to T_t , the transition temperature from the Sb-rich $c(4 \times 4)$ to the asymmetric (1×3) , F is close to unity and the pattern appears as a symmetric (1×3) . However, this symmetric structure was not observed under the static conditions used in the present work. This is perhaps not too surprising since de Oliveira *et al.*³¹ also concluded that the disordered nature of this surface means that any structural model for the surface cannot be based solely on removing one or two rows from a regular array, as shown in Fig. 11, as this would result in a symmetric and ordered diffraction pattern only observed, and sustained, under specific MBE growth conditions of controlled III/V arrival rate at the surface.

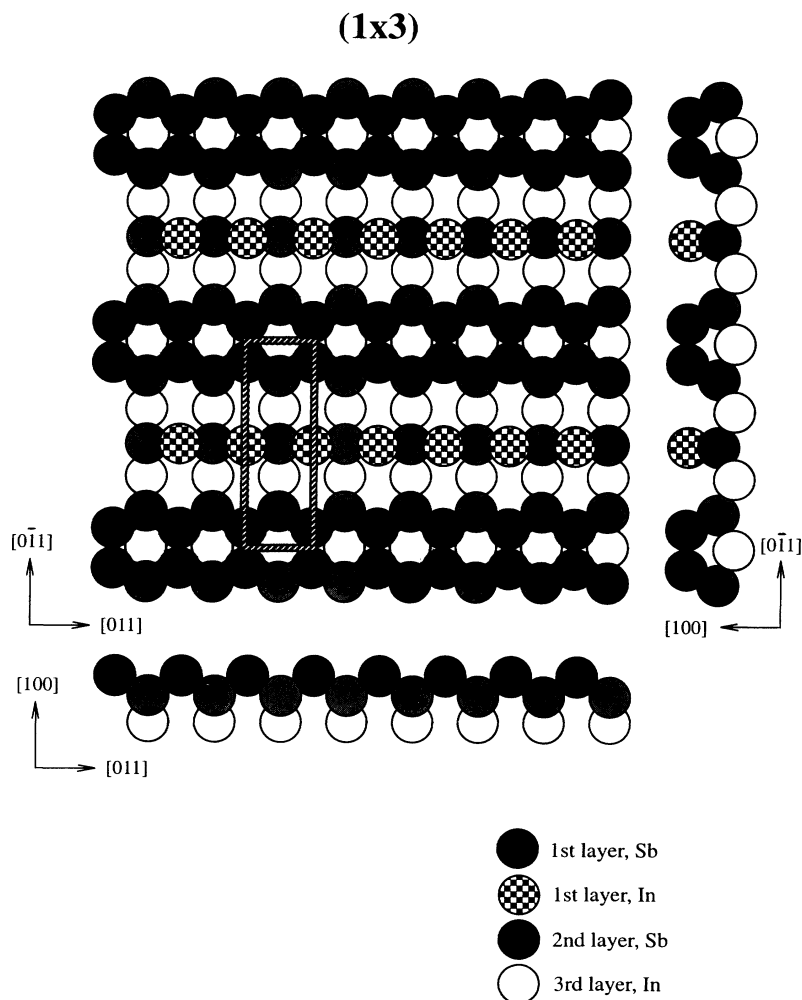


FIG. 11. A model of the asymmetric- (1×3) surface, originally proposed by Franklin *et al.* (Ref. 32) for the related GaSb(100)- (1×3) surface, and adapted for InSb(100), showing the plan view and the side view of the structure. The (1×3) unit cell is indicated on the plan view.

D. Coexistence and the (4×3) surface

Following annealing of any of the Sb-rich reconstructions, the Sb desorbs and the overall concentration on the surface decreases as the structure changes from (1×1) , to $c(4 \times 4)$ and finally to asymmetric (1×3) . This method was used in particular to form the asymmetric (1×3) surface from the $c(4 \times 4)$. On occasion, a mixed LEED pattern was observed when the substrate was annealed to a temperature somewhere in the region of T_i . However, investigation of this $c(4 \times 4)/(1 \times 3)$ mixed surface with the STM indicated that only the $c(4 \times 4)$ reconstruction was present over wide areas of the surface, although the number of Sb-dimer blocks with one or more missing atoms was significantly increased.

Further increases in the annealing temperature resulted in the asymmetric (1×3) until, at still higher temperatures (> 625 K), the surface loses Sb by desorption and tends towards the In-rich $c(8 \times 2)$ surface onto which the initial Sb deposition occurred. Following an extended anneal at this temperature, the LEED patterns observed exhibited a sharp $c(8 \times 2)$ structure indicating an ordered In-terminated surface. The STM images of this surface, however, showed regions of coexistence of the asymmetric (1×3) and $c(8 \times 2)$ reconstructions. Figure 12 shows a grey-scale STM topograph of one such region. The image ($265 \times 110 \text{ \AA}^2$) shows the Sb chains of the asymmetric (1×3) structure aligned approximately along the $[011]$ direction and the double rows of bright dots from second layer Sb lone pairs associated with the $c(8 \times 2)$ structure. Sharp boundaries or transitions are observed between these regions in the $[011]$ direction, and also along the $[0\bar{1}1]$ direction where the (1×3) intrudes into regions of the $c(8 \times 2)$ structure. This coexistence is perhaps not too surprising since, although these regions were frequently observed, they were not evenly distributed over the whole of the sample. Hence their formation

is most likely due to small temperature variations across the sample during annealing, which is not unusual with the radiative heating system being used.

It has also been proposed that the (4×3) reconstruction, observed across a range of temperatures in a very narrow band around a 1:1 flux ratio or static Sb/In concentration (see Fig. 1), is not in fact an independent structure but a mixture of domains of the asymmetric (1×3) and $c(8 \times 2)$ reconstructions.¹² This reconstruction has previously been identified during MBE growth,^{10,11} and there is evidence that at temperatures above approximately 650 K the (4×3) appears to merge with the asymmetric (1×3) .¹¹ Throughout the course of this work, however, it was not possible to produce either a (4×3) or pseudo- (4×3) LEED pattern, which tends to support the premise that the (4×3) is indeed a mixed domain structure.

E. The (1×1) surface

The (1×1) reconstruction of the InSb(100) surface is the most Sb rich of all the reconstructions stable under static conditions. It is also the bulk structure at the lowest growth temperatures consistent with epitaxy.¹¹ The LEED pattern is shown in Fig. 2(d) and a grey-scale STM image ($175 \times 150 \text{ \AA}^2$) of the (1×1) structure is shown in Fig. 13. The image shows chains of Sb atoms aligned along the $[011]$ direction in a similar manner to the asymmetric (1×3) reconstruction shown in Fig. 13. In fact, despite the difference in the LEED patterns of the two reconstructions [Figs. 2(c) and 2(d)], the local or short-range ordering of the Sb atoms observed with the STM is very similar. However, over an area of several hundred \AA , there is a considerable degree of disorder in the surface, particularly when compared to the $c(8 \times 2)$ and $c(4 \times 4)$ structures. Photoemission data from John,

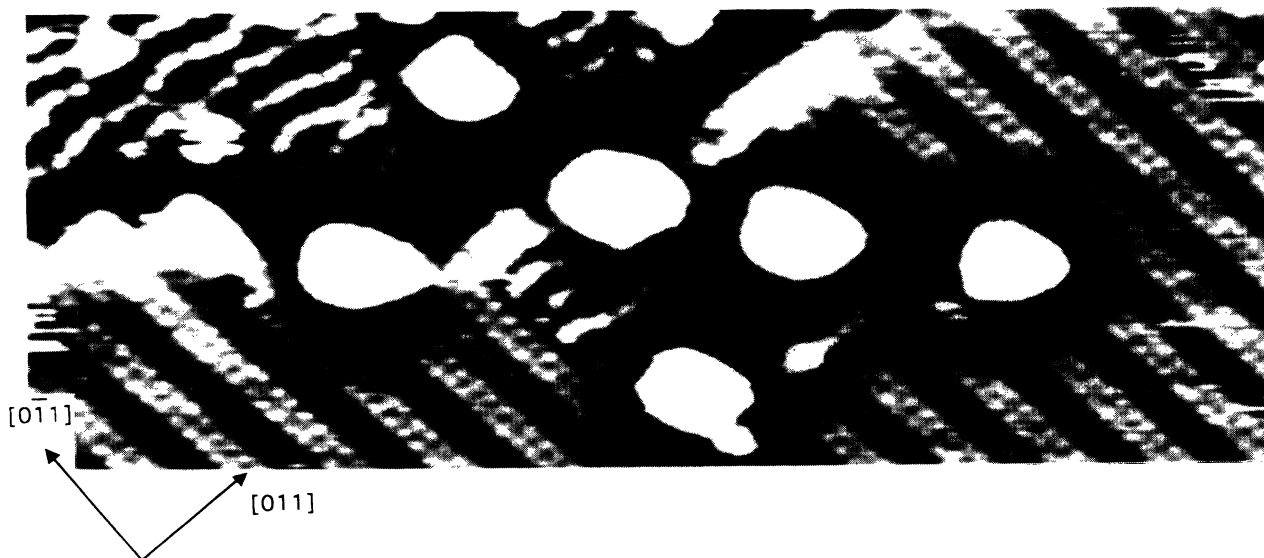


FIG. 12. A wide-area scan ($265 \times 110 \text{ \AA}^2$) grey-scale topographic image demonstrating the coexistence of the $c(8 \times 2)$ and asymmetric (1×3) structures. This was observed following annealing of the asymmetric- (1×3) structure to ~ 600 K. As discussed in the text, a mixture of domains of these two structures is responsible for the formation of the (4×3) reconstruction observed for equal fluxes (1:1 ratio) of In and Sb. The image was recorded with a bias voltage of -2.5 V and a tunnel current of 1 nA.

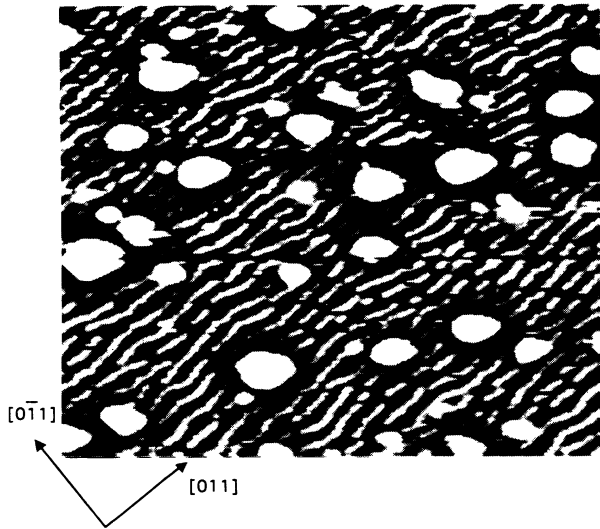


FIG. 13. A wide-area scan ($175 \times 150 \text{ \AA}^2$) grey-scale topographic image of the disordered (1×1) surface showing the Sb atoms aligned in short chains along the $[011]$ direction. The image was recorded with a bias voltage of -2.5 V and a tunnel current of 1 nA .

Miller, and Chiang¹² indicate that both the (1×1) and asymmetric (1×3) surfaces are extremely Sb rich (i.e., greater than 1.5 ML of Sb on the surface), and that the (1×1) surface contains the greater amount of Sb. These authors also claim to have observed a symmetric (1×3) in the same region of the phase diagram as the (1×1) . Such a reconstruction was not observed in the present study, although the existence of such a structure can be explained in terms of mixed domains (discussed in Sec. III C). Also, no evidence of the very Sb-rich (7×5) structure, on the boundary between the (1×1) and $c(4 \times 4)$ regions, was observed. The most likely reason for this is the instability of such a structure that only exists for Sb/In flux ratios in excess of 7:1.

IV. CONCLUSIONS

Atomic resolution STM has been used to study a number of the surface reconstructions formed on InSb(100).

The In-terminated $c(8 \times 2)$ structure was prepared by cycles of ion bombardment and annealing to temperatures of about 650 K . Large atomically flat, ordered areas ($1000 \times 1000 \text{ \AA}^2$) of the surface were produced in this manner, and high-resolution filled-states STM images of this surface indicate a (4×1) unit cell. This (4×1) periodicity and the $c(8 \times 2)$ translational symmetry observed by LEED are consistent with a structural model in which $\frac{3}{4} \text{ ML}$ of In dimers are located in the topmost surface layer above an Sb-terminated second layer. The (4×1) structure in STM arises from tunneling from occupied lone-pair orbitals of exposed second-layer Sb atoms.

The deposition of Sb_4 onto the InSb(100)- $c(8 \times 2)$ surface led to the formation of a number of Sb-terminated reconstructions depending on the temperature of the surface at which the deposition was carried out, or alternatively the annealing temperature after formation of a Sb-rich surface. Structures produced in this way include $c(4 \times 4)$, (1×1) , and asymmetric (1×3) . In certain cases, coexistence of some of these structures was observed both by LEED and STM. Both the (1×1) and asymmetric (1×3) surfaces display a considerable degree of local disorder, while the $c(4 \times 4)$ surface is highly ordered. High-resolution images of the $c(4 \times 4)$ surface reveal a surface layer consisting of blocks of six Sb atoms, which form three sets of so-called dimers. The images are consistent with a structural model in which the top layer of Sb atoms are bonded to an already Sb-terminated surface. The dimers formed on this structure are therefore fundamentally different from those formed on the other Sb-terminated reconstructions, in that the Sb atoms in the surface layer are bonded to three other Sb atoms, with the bonding being more characteristic of bulk amorphous antimony.

ACKNOWLEDGMENTS

The SERC (U.K.) are thanked for the financial support of this work and providing research studentships for TCQN and SMD. Tom Parker is also thanked for help with some data transfer associated with the STM figures presented in this paper.

*Corresponding author: FAX: 44-203-692-016. Electronic address: spcm@spec.warwick.ac.uk

†Present address: Department of Physics, University of Warwick, Coventry CV4 7AL, U.K.

¹S. R. Kurtz, G. C. Osbourn, R. M. Beilfeld, L. R. Dawson, and H. J. Stein, Appl. Phys. Lett. **52**, 831 (1988).

²R. G. van Welzenis and B. K. Ridley, Solid State Electron. **27**, 113 (1984).

³T. Ashley, A. B. Dean, C. T. Elliott, C. F. McConville, G. J. Pryce, and C. R. Whitehouse, Appl. Phys. Lett. **59**, 1761 (1991).

⁴T. S. Jones, M. Q. Ding, N. V. Richardson, and C. F. McCon-

ville, Appl. Surf. Sci. **45**, 85 (1990).

⁵T. S. Jones, M. Q. Ding, N. V. Richardson, and C. F. McConville, Surf. Sci. **247**, 1 (1991).

⁶M. O. Schweitzer, M. Q. Ding, N. V. Richardson, T. S. Jones, and C. F. McConville, J. Phys. Condens. Matter **3**, S271 (1991).

⁷W. T. Yuen, M. O. Schweitzer, T. S. Jones, C. F. McConville, E. A. Johnson, A. Mackinnon, N. V. Richardson, and R. A. Stradling, Semicond. Sci. Technol. **8**, S396 (1993).

⁸D. P. Woodruff and K. Horn, Vacuum **33**, 633 (1983).

⁹R. G. Jones, N. K. Singh, and C. F. McConville, Surf. Sci. **208**, L34 (1989).

- ¹⁰K. Oe, S. Ando, and K. Sigiyama, *Jpn. J. Appl. Phys.* **19**, L417 (1980).
- ¹¹A. J. Noreika, M. H. Francombe, and C. E. C. Wood, *J. Appl. Phys.* **52**, 7416 (1981).
- ¹²P. John, T. Miller, and T. C. Chiang, *Phys. Rev. B* **39**, 1730 (1989).
- ¹³B. F. Mason, S. Laframboise, and B. R. Williams, *Surf. Sci.* **258**, 279 (1991).
- ¹⁴B. F. Mason and B. R. Williams, *Surf. Sci.* **243**, 1 (1991).
- ¹⁵M. O. Schweitzer, F. M. Leibsle, T. S. Jones, C. F. McConville, and N. V. Richardson, *Surf. Sci.* **280**, 63 (1993).
- ¹⁶D. K. Biegelsen, R. D. Bringans, J. E. Northrup, and L. E. Schwartz, *Phys. Rev. B* **41**, 5701 (1990).
- ¹⁷V. Bressler-Hill, M. Wassermeier, K. Pond, R. Maboudian, G. A. D. Briggs, P. M. Petroff, and W. H. Weinberg, *J. Vac. Sci. Technol. B* **10**, 1881 (1992).
- ¹⁸M. C. Gallagher, R. H. Prince, and R. F. Willis, *Surf. Sci.* **275**, 31 (1992).
- ¹⁹M. D. Pashley, K. W. Haberen, W. Friday, J. M. Woodall, and P. D. Kiorchner, *Phys. Rev. Lett.* **60**, 2176 (1988).
- ²⁰R. M. Feenstra, J. A. Stroscio, J. Tersoff, and A. P. Fein, *Phys. Rev. Lett.* **58**, 1192 (1987).
- ²¹L. J. Whitman, J. A. Stroscio, R. A. Dragoset, and R. J. Celotta, *J. Vac. Sci. Technol. B* **9**, 770 (1991).
- ²²F. D. Auret, *J. Electrochem. Soc.* **129**, 2752 (1982).
- ²³M. O. Schweitzer, F. M. Leibsle, T. S. Jones, C. F. McConville, and N. V. Richardson, *Semicond. Sci. Technol.* **8**, S342 (1993).
- ²⁴C. F. McConville, T. S. Jones, F. M. Leibsle, and N. V. Richardson, *Surf. Sci.* **303**, L373 (1994).
- ²⁵S. L. Skala, J. S. Hubacek, J. R. Tucker, J. W. Lyding, S. T. Chou, and K. Y. Cheng, *Phys. Rev. B* **48**, 9138 (1993).
- ²⁶I. Tanaka, S. Ohkouchi, T. Kato, and F. Osaka, *J. Vac. Sci. Technol. B* **9**, 2277 (1991).
- ²⁷P. K. Larsen, J. H. Neave, J. F. van der Veen, P. J. Dobson, and B. A. Joyce, *Phys. Rev. B* **27**, 4966 (1983).
- ²⁸M. Wassermeier, V. Bressler-Hill, R. Maboudian, K. Pond, X. S. Wang, W. H. Weinberg, and P. M. Petroff, *Surf. Sci.* **278**, L147 (1992).
- ²⁹H. Norenberg and N. Koguchi, *Surf. Sci.* **292**, 199 (1993).
- ³⁰A. R. Avery, D. M. Holmes, J. Sudijono, T. S. Jones, and B. A. Joyce, *Surf. Sci.* (to be published).
- ³¹A. G. de Oliveira, S. D. Parker, R. Droopad, and B. A. Joyce, *Surf. Sci.* **227**, 150 (1990).
- ³²G. E. Franklin, D. H. Rich, A. Samsavar, E. S. Hirschorn, F. M. Leibsle, T. Miller, and T. C. Chiang, *Phys. Rev. B* **41**, 12 619 (1990).

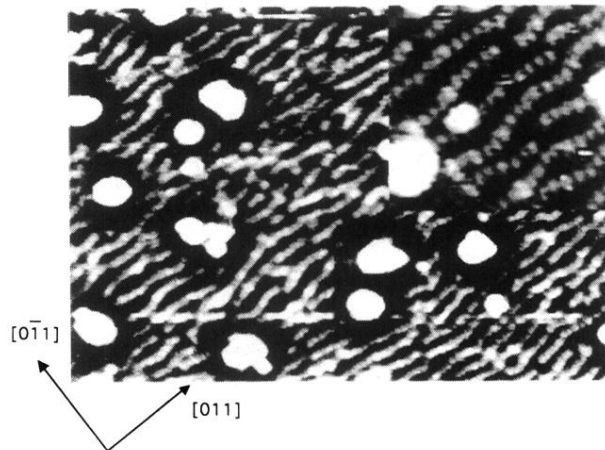


FIG. 10. A wide-area scan ($200 \times 130 \text{ \AA}^2$) grey-scale topographic image of the asymmetric- (1×3) surface showing the Sb atoms aligned in short, "wormlike" chains along the $[011]$ direction. The high-resolution inset ($80 \times 50 \text{ \AA}^2$) clearly shows the individual Sb atoms within each chain. The image was recorded with a bias voltage of -2.75 V and a tunnel current of 1 nA .

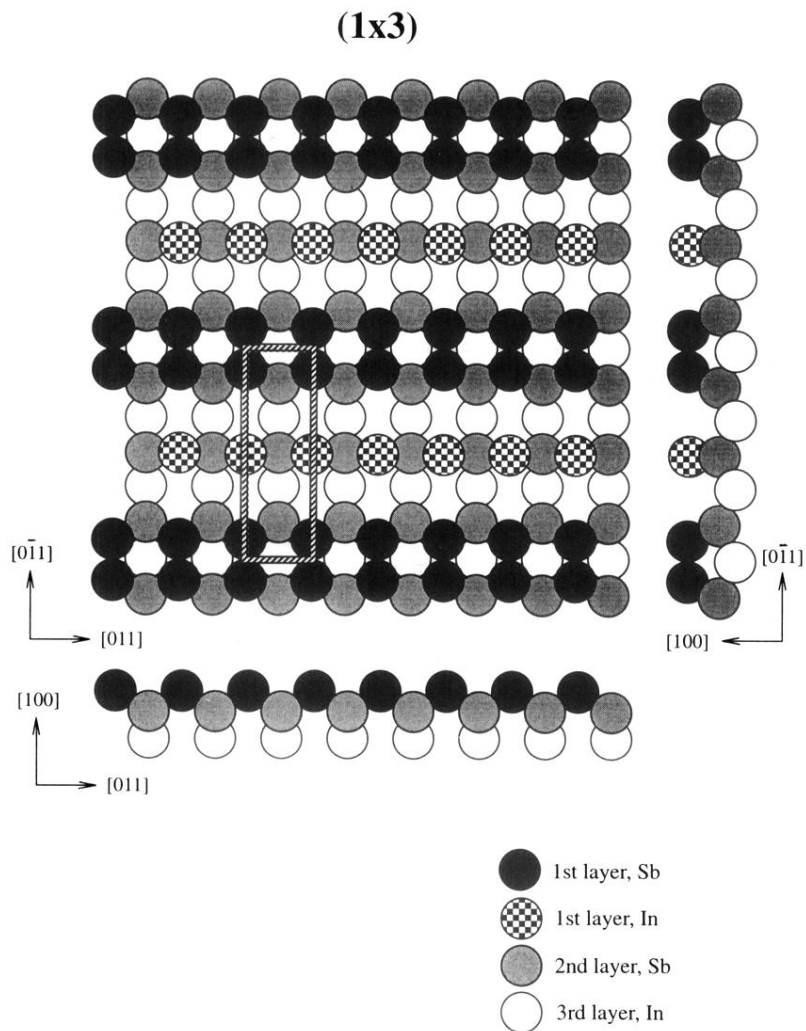


FIG. 11. A model of the asymmetric-(1×3) surface, originally proposed by Franklin *et al.* (Ref. 32) for the related GaSb(100)-(1×3) surface, and adapted for InSb(100), showing the plan view and the side view of the structure. The (1×3) unit cell is indicated on the plan view.

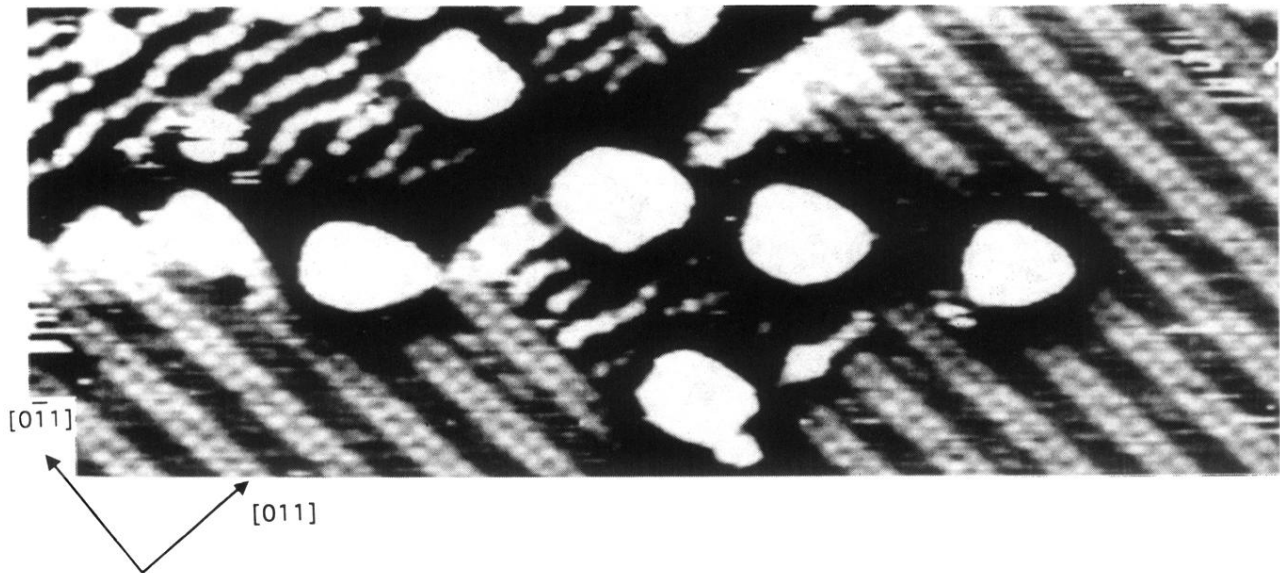


FIG. 12. A wide-area scan ($265 \times 110 \text{ \AA}^2$) grey-scale topographic image demonstrating the coexistence of the $c(8 \times 2)$ and asymmetric (1×3) structures. This was observed following annealing of the asymmetric- (1×3) structure to $\sim 600 \text{ K}$. As discussed in the text, a mixture of domains of these two structures is responsible for the formation of the (4×3) reconstruction observed for equal fluxes (1:1 ratio) of In and Sb. The image was recorded with a bias voltage of -2.5 V and a tunnel current of 1 nA .

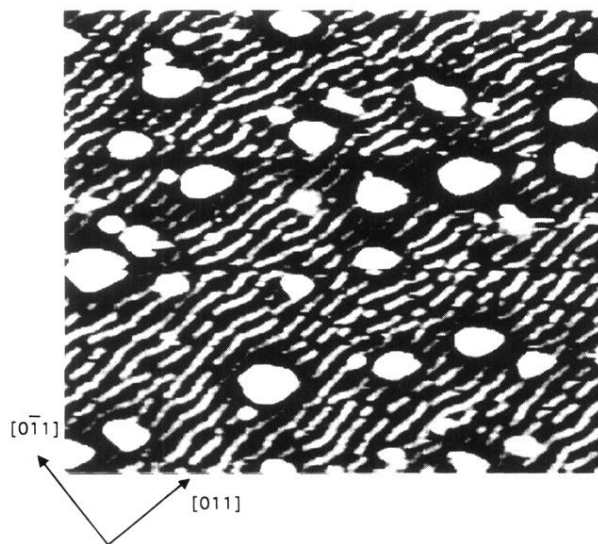


FIG. 13. A wide-area scan ($175 \times 150 \text{ \AA}^2$) grey-scale topographic image of the disordered (1×1) surface showing the Sb atoms aligned in short chains along the $[011]$ direction. The image was recorded with a bias voltage of -2.5 V and a tunnel current of 1 nA .

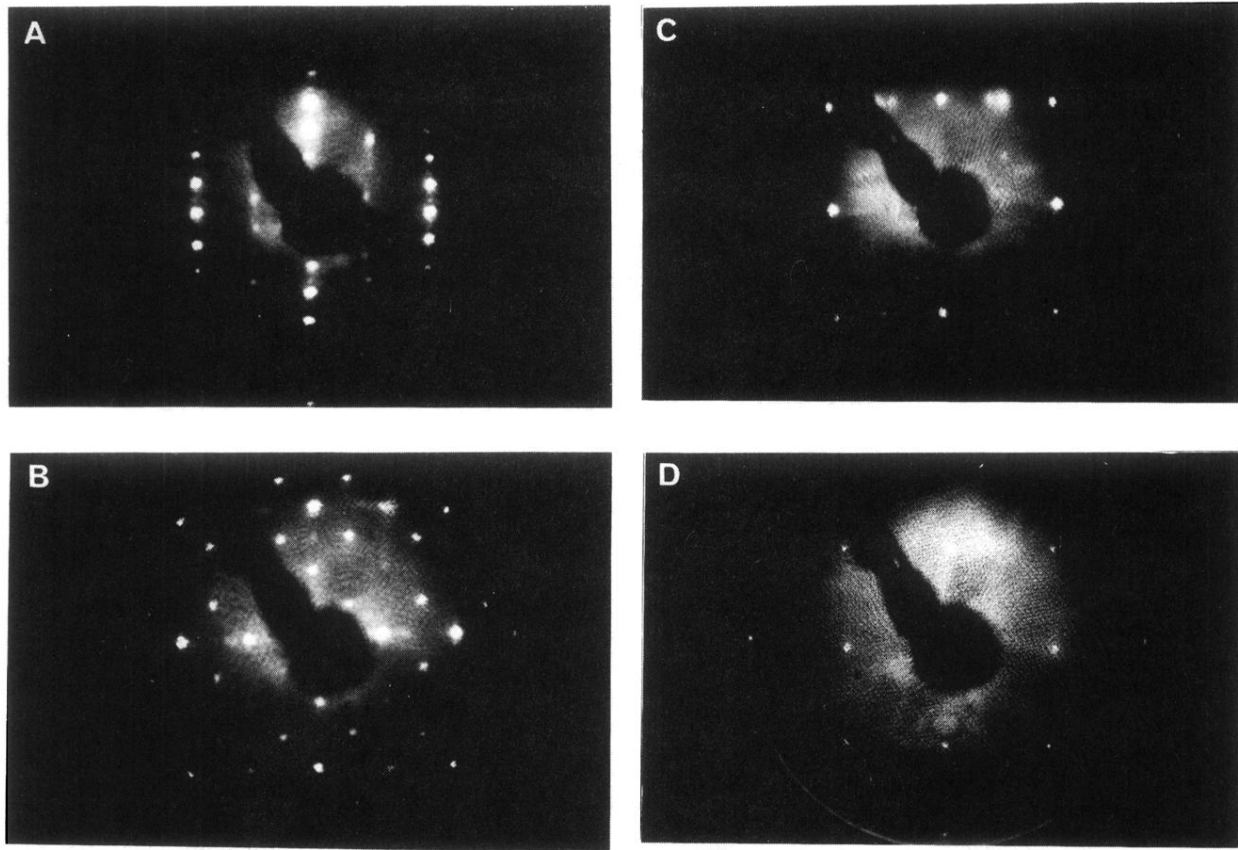


FIG. 2. LEED patterns of the various reconstructions formed on InSb(100): (a) the In-terminated $c(8 \times 2)$, and the Sb-terminated surfaces (b) $c(4 \times 4)$, (c) asymmetric (1×3) , and (d) (1×1) . The primary electron energy in each case was 47 eV.

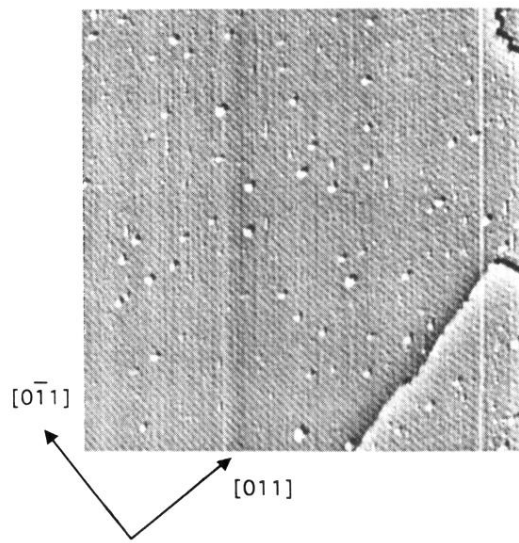


FIG. 3. A grey-scale STM topographic image ($1500 \times 1500 \text{ \AA}^2$) of the $\text{InSb}(100)\text{-}c(8 \times 2)$ surface produced after three cycles of argon-ion sputtering and annealing (650 K). Note the In droplets formed as a result of the ion bombardment. This image was produced using a sample bias of -2 V and a tunneling current of 1 nA .

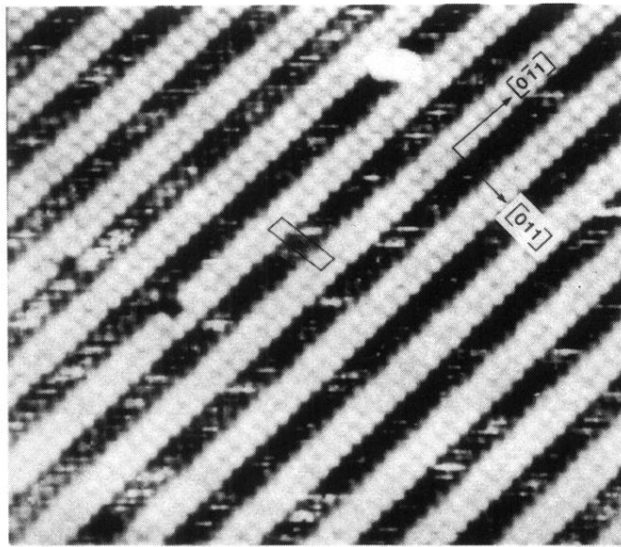


FIG. 4. A grey-scale STM topographic image ($200 \times 200 \text{ \AA}^2$) of the InSb(100)- $c(8 \times 2)$ surface after three cycles of argon-ion sputtering and annealing (650 K). The visible double rows are the occupied lone pair orbitals of second-layer Sb atoms. The (4×1) unit cell is indicated in the image which was recorded with a sample bias of -3 V and a tunneling current of 1 nA .

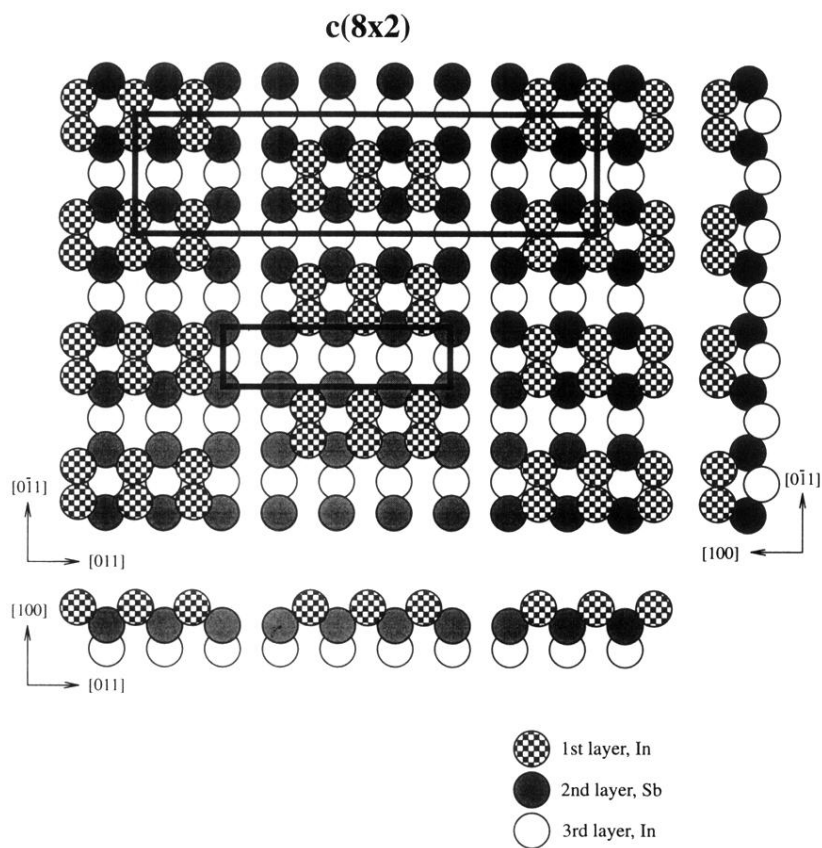


FIG. 5. A structural model for the InSb(100- $c(8 \times 2)$) surface reconstruction. The (4×1) unit cell refers only to the Sb atoms in the second layer visible in the STM image, while the $c(8 \times 2)$ translational symmetry as seen by LEED takes into consideration the In dimers in the topmost surface layer.

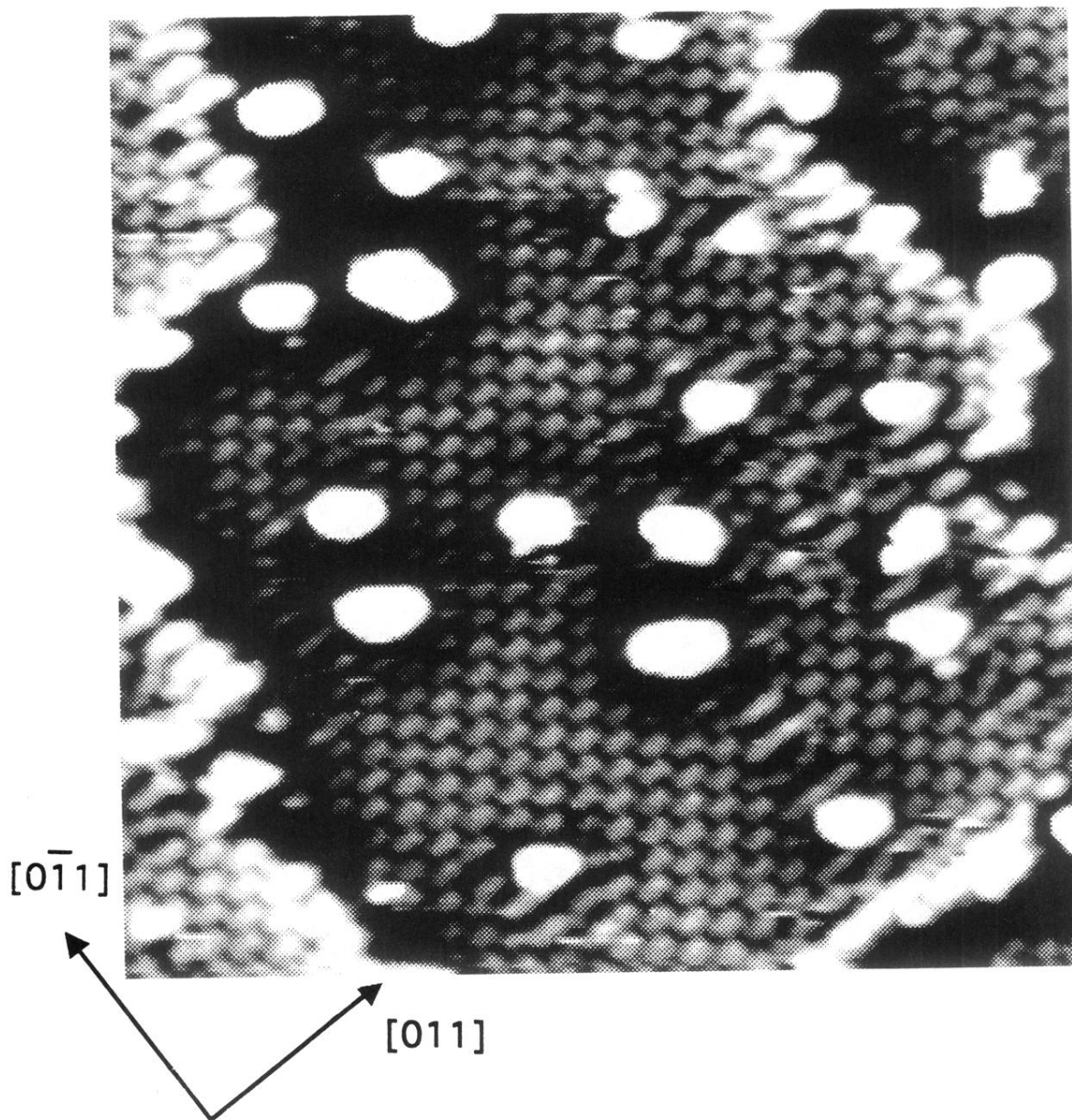


FIG. 6. A filled-states image ($400 \times 400 \text{ \AA}^2$) of the InSb(100)- $c(4 \times 4)$ surface, prepared by Sb_4 deposition onto the InSb(100)- $c(8 \times 2)$ surface held at a temperature of $\sim 500 \text{ K}$. Note the “bricklike” blocks which are identified as Sb dimers. The image was recorded with a sample bias of -2.5 V and a tunnel current of 1 nA .

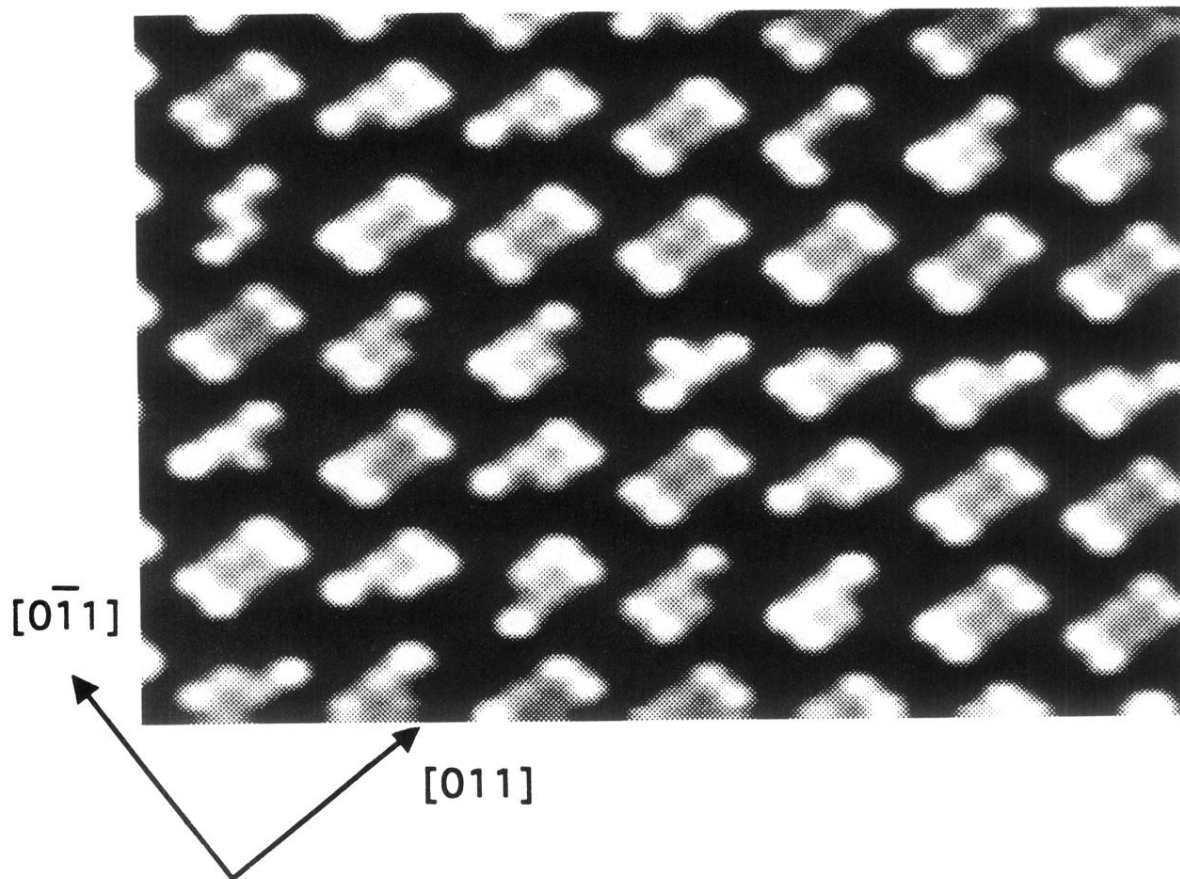


FIG. 7. A high-resolution filled-states image ($105 \times 70 \text{ \AA}^2$) of the InSb(100)- $c(4 \times 4)$ surface showing the individual Sb atoms arranged in blocks of three dimers separated by a missing dimer. The $c(4 \times 4)$, or $(2\sqrt{2} \times 2\sqrt{2})R45^\circ$, unit cell can clearly be seen by comparison with the model shown in Fig. 9. The image was recorded with a sample bias of -2.5 V and a tunneling current of 1 nA .

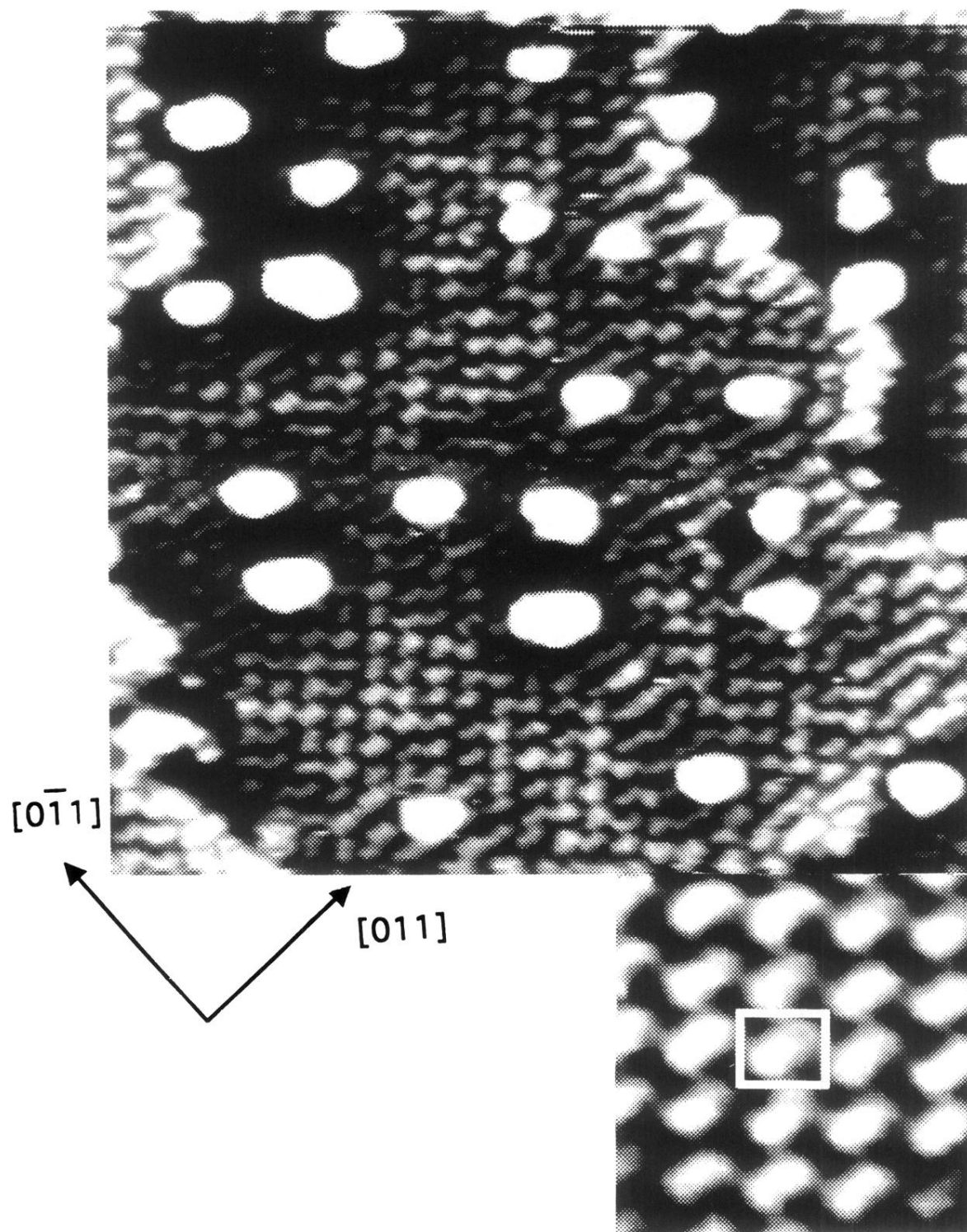


FIG. 8. An empty-states image ($400 \times 400 \text{ \AA}^2$) of the InSb(100)-c(4×4) surface, again showing Sb dimers arranged in blocks of three separated by a missing dimer. Note that the blocks, although identifiable, are less well resolved than in Fig. 7, even though the image was taken over the same area. The inset shows a region of the same surface at higher resolution. The image was recorded with a sample bias of +2.5 V and a tunneling current of 1 nA.

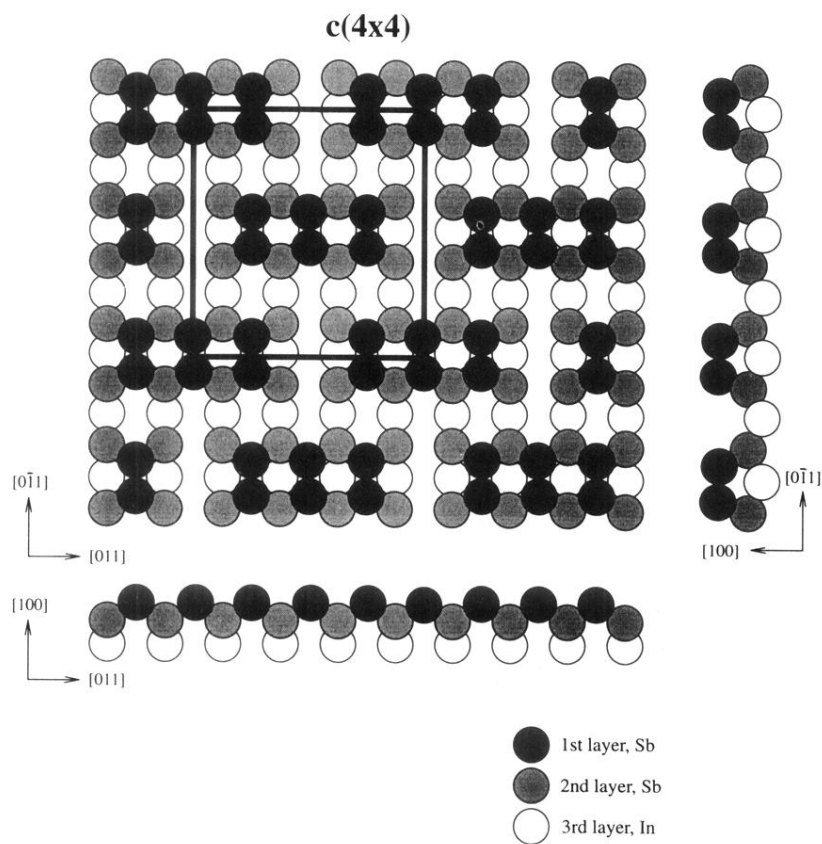


FIG. 9. A structural model for the Sb-terminated InSb(100)- $c(4 \times 4)$ surface. The model consists of 0.75-ML Sb atoms chemisorbed onto a full monolayer of Sb terminating the surface.